Third International Conference on Sustainable Construction Materials and Technologies http://www.claisse.info/Proceedings.htm

CHARACTERIZATION OF ALKALI ACTIVATED SLAG GEL USING NANO-INDENTATION

Berhan S. Gebregziabiher[1] and Sulapha Peethamparan[2*]

[1]Doctoral Graduate Student, Department of Civil and Environmental Engineering, Clarkson University, Potsdam, NY 13699, USA, Email: gebregbs@clarkson.edu

[2*]Assistant Professor, Department of Civil and Environmental Engineering, Clarkson University, Potsdam, NY 13699, USA. Email: speetham@clarkson.edu; Phone: 001-315-268-4435; Fax: 001-315-268-7985. Corresponding Author and speaker.

ABSTRACT

Characterization of alkali activated slag gel using nano-indentation is reported in this paper. Ground granulated blast furnace slag is activated with different concentrations of sodium hydroxide and sodium silicate activating solutions. The activated slag pastes are cured at 23±2^{o}C for 28 days in sealed plastic containers. The resulting hardened alkali activated pastes are impregnated with epoxy and then polished. The microstructures of the polished pastes were characterized using a scanning electron microscope under the backscattered mode. Three distinct phases were identified in the microstructure of the sodium hydroxide activated paste (outer products, inner products, and unreacted slag grains); only two phases were identified in the sodium silicate activated slag system (outer products and unreacted slag grains). The nano-scale deformation of various phases found in the hardened alkali activated paste is measured using a TI-950 TriboIndenter, and the corresponding hardness and the reduced modulus was determined.

Key Words: alkali activated slag**,** microstructure, nano-indentation, reduced modulus, hardness

INTRODUCTION

Ground granulated blast furnace slag (GGBFS, or “slag”) has been used as a supplementary cementitious material (SCM) to enhance the fresh and hardened properties of concrete for many years (Lothenbach, 2011; Monteiro, 2006). In order to further increase the sustainability of concrete production, significant research focus has recently shifted towards the development of cement free binders using slag as the sole binder. This technology relies on the alkali activation of otherwise latent hydraulic slag. The alkali activated systems have been evaluated by many researchers and substantial progress has been made in its development (Wang, 1995; Scrivener, 2011).

The most commonly used alkalis for activating slag are sodium hydroxide, sodium carbonates, and sodium silicates. The main factors that affect the activation process are the amount of sodium oxide (%Na_2O) and the silica modulus (SiO_2/ Na_2O) of the solution (Fernadez- Jimenez,

2005; Fernadez- Jimenez, 1999; Shi, 1996; Ben Haha, 2010). The microstructure development, the composition of the new products, and nano-mechanical properties of the new products formed all depend on the type and dosage of the activator used. The main reaction products, as suggested by many researchers, are calcium silicate hydrate (C-S-H) and hydrotalcite –like products ($Mg_6Al_2(CO_3)(OH)_{16}.4(H_2O)$) (Ben Haha, 2011; Ben Haha, 2012; Wang, 1995). The nano-mechanical property evaluation of the alkali activated binder gel is important for developing an understanding of the characteristics of the binding gel. This type of characterization allows the determination of the mechanical properties of the heterogeneous component phases in the activated slag gel by determining the hardness and reduced modulus of individual phases at different indentation points in the system (Sakulich, 2011; Miller, 2008; Davydov, 2011)

In this paper, the nano-mechanical properties of different phases identified in a system of alkali activated slag pastes were characterized using a TI-950 TriboIndenter. The effect of two types of activators and their concentration on the microstructure of alkali activated slag pastes cured for 28 days under ambient conditions were examined using a scanning electron microscope.

MATERIALS

A grade 100, ASTM C 989 compliant, ground granulated blast furnace slag was used as the starting material in this study. The oxide chemical composition of the slag was 36% SiO_2, 10.5% Al_2O_3, 39.8% CaO, 7.93% MgO, 0.27% Na_2O, 2.11% SO_3, 0.16% K_2O and 0.67% Fe_2O_3. The Si/Al, the Blaine surface area, and loss on ignition were 3.428, 340 m^2/kg and 3%, respectively. The particle size distribution, determined using a laser particle size analyzer, showed that 80% of the particles had a size lower than 10 μm with an average particle size of 7.5 μm.

The alkali activators, both commercially available, were sodium hydroxide (NaOH) pellets and a solution of sodium silicate hydrate (NSH), commonly known as *waterglass*. Required quantities of NaOH were dissolved in deionized water to make 5, 8 and 12M solutions. NSH activator was used for formulating solutions with two different silica moduli (Na_2O/SiO_2, SM), 1.5 and 2.5. The Na_2O content was kept constant at 2.5% by mass of slag.

EXPERIMENTAL METHODS

Sample Preparation

Alkali activated binder mixtures were prepared using slag as the starting material and NaOH or sodium silicate hydrate solution as the activator. All the pastes were prepared with solution to slag ratio of 0.5 (by mass). Alkaline solutions of the desired concentration were prepared and allowed to cool to room temperature prior to mixture preparation. After measuring the right amounts of solution and slag, the solution was poured into the mixing bowl. With the mixer running at a low speed, the slag was slowly added into the bowl within 30 seconds. The mixing was continued at low speed for one more minute followed by a 30 second rest. While the mixer was at rest, unmixed slag was scraped from the sides of the bowl. Finally, one additional minute of high-speed mixing was performed to obtain a uniform mixture. Small cylindrical specimens were prepared in plastic vials for preparing the SEM samples. Cubic samples of dimension

2x2x2 inches were also prepared for determining the compressive strength. Both sets of samples were compacted on a vibrating table and finished. The finished samples were stored in sealed plastic containers in a curing room with controlled relative humidity at approximately 99.9% and temperature at 23±2^{o}C. Compressive strength of activated slag paste binder was determined after 28 days of curing as per ASTM standard.

Scanning Electron Microscopy (SEM) Examination

The samples prepared in small plastic vials were cured for 28 days, they were cut using a slow speed saw (Iso-Cut) to the desired size, soaked in iso-propanol to quench the reaction and subsequently oven dried at 50 ^{o}C for three days. The specimens were then impregnated with epoxy and polished to a very smooth surface appropriate for Back Scattered Electron mode of SEM (BSE-SEM) examination and nano-indentation. The specimen preparation protocol used in the study is reported elsewhere (Diamond, 2006). For BSE-SEM, the samples were sputter coated using 60% Gold (Au) and 40% Palladium (Pd) to create a conductive layer over the surface. The scanning electron microscope used was a JEOL JSM-7400F electron microscope and was operated in its back-scattered mode.

The microstructure of the 28 day old hardened alkali activated slag pastes were examined under the backscattered mode of the SEM. A number of images at various magnifications were collected from each sample and analyzed to determine the various material phases and other microstructural features as a function of the type and concentration of the activating solution.

Nano Indentation

The polished samples, as prepared in the previous section, were indented using a TI 950 Tirbo-Indenter to determine the reduced elastic modulus and hardness. The mechanical properties of the different phases at the micron and submicron levels were studied. The procedure consists of establishing contact between the sample and the indenter with known parameters and geometry. The testing was performed in a load controlled mode, in which the force was applied as the control variable through a preset program with loading, holding and unloading periods. This mode utilizes a feedback loop between the transducer controller and transducer to precisely achieve the desired force or displacements during the tests. A trapezoidal load cycle was used, consisting of a linear ramp from 0 to 4mN over 10 s, followed by a 5 second hold, and then uniform unloading over 10 s. Analysis of the indentation results was performed based on the Oliver-Pharr method. The indenter probe used was the Berkovich tip with elastic modulus of 1140 GPa and Poisson's ratio of 0.07.

The contact radius, a, is related to the indenter load P, the indenter tip radius R, and the elastic properties of the contacting materials.

$$a^3 = \frac{3PR}{4E_r} \quad (1)$$

Where E_r combines the elastic modulus of the indenter and the specimen and is often referred to as the reduced modulus. The reduced modulus can be related to the modulus of the indenter, $E,'$ and elastic modulus of the specimen, E, by:

$$\frac{1}{E_r} = \frac{(1 - \mathrm{J}^2)}{E} + \frac{(1 - j'^2)}{E'} \quad (2)$$

Where *J* is the Poisson's ratio of the specimen and *J'* is the Poisson's ratio of the indenter.
The hardness is given by:

$$H = \frac{Pmax}{A} \quad (3)$$

Where, P_{max} is the maximum indentation force and *A* is the projected contact area corresponding to the maximum load.
The reduced modulus,

$$E_r = \frac{(S\sqrt{\pi})}{2\sqrt{A}} \quad (4)$$

Where, *S* is the stiffness of the unloading curve. E_r was obtained using 95-30% of the unloading curves of the data points.

RESULTS

Compressive Strength

The compressive strength of slag paste activated with NaOH and NSH solutions was determined after 28 days of curing. The compressive strength of the NaOH activated paste was approximately 30 MPa, irrespective of the concentration of the activating solution. On the contrary, SM of the NSH solution had a substantial influence on the 28-day compressive strength. Compressive strengths of 40 MPa and 70 MPa were obtained for 1.5 and 2.5 SM NSH activated paste, respectively.

Microstructure of NaOH activated slag system

Microstructure developed in 28 day old 5, 8 and 12M NaOH-activated slag systems is shown in Fig 1(a), (b) and (c), respectively. In general, the microstructure had four easily distinguishable phases; 1) very bright unreacted slag grains, 2) a thin reaction ring around the slag grains (inner product), 2) darker gray shaded completely reacted small slag grains, 3) a ground mass gel (outer products) with a lighter gray shade compared to the completely reacted slag grains and 4) the black region representing pores. These phases are clearly marked in Fig. 1(d). The reaction ring shell was formed around the slag grains in all concentrations indicating that the hydration process is mainly diffusion controlled. It can also be noted that as the activating solution concentration increases, the reaction ring thickness decreases. The thickness of the rings around the slag grains was 1.8-2, 1.2-1.5 and 1.0-1.25 micrometers for 5, 8 and 12 M activated systems, respectively. The thickness of the ring was measured from a number of slag grains and the average was taken for each case

Microstructure of NSH Activated Slag System

The microstructure of 28- day old hardened 1.5 and 2.5 silica modulus NSH activated slag systems are shown in Fig. 2. There was no significant difference in the microstructure between these two samples. However, the microstructure of NSH activated slag systems was quite

different from that of the NaOH activated system. The reaction ring around slag grains was absent in NSH activated slag systems. Therefore, the unreacted slag grains and the ground mass gel (the outer product) were the only two easily distinguishable phases in NSH activated slag systems.

The SEM micrographs presented in Fig. 1 and 2, and several other micrographs not presented here, showed the presence of numerous microcracks in both NaOH and NSH activated systems with slightly more cracks in the latter compared to the former. Further research is needed to determine the cause and mechanism of cracking in alkali activated slag systems.

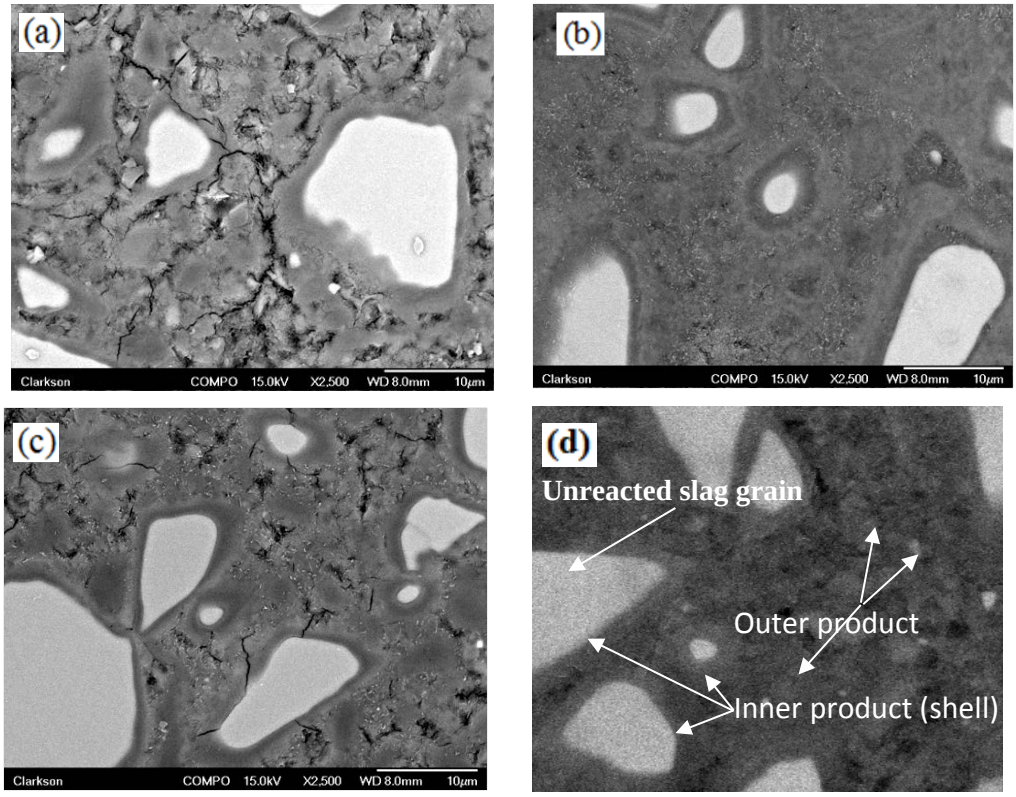

Fig. 1: (a) 5M (b) 8M and (c) 12M NaOH activated slag after 28 days curing (d) different phases present in the microstructure

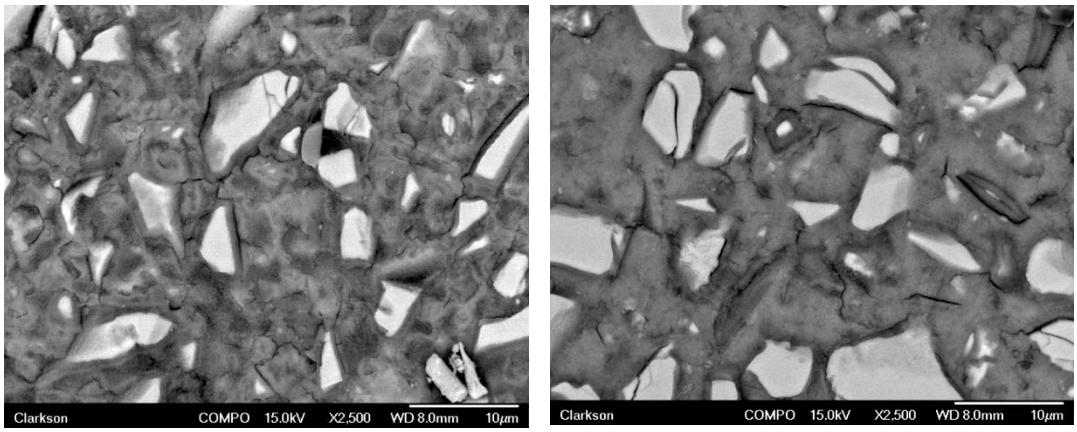

Fig. 2: Microstructure of (a) 1.5 silica modulus (b) 2.5 silica modulus NSH activated slag after 28 days of curing

Nano-Mechanical Properties

Automated indentations (statistical nano-indentation) were conducted on a set of pre-defined grid points with spacing of 4μm on the selected locations of polished samples. A typical pattern is shown in Fig. 3. In all the cases, the locations were selected in such a way that a similar size slag grain was obtained. A single location in a given grit pattern had 100 points. Three such locations were studied on each sample. Thus, a total of 300 indentation load-depth curves were collected and analyzed for a single sample. In addition to automated indentation, several manual indentations on selected points were also conducted. The data obtained was analyzed to estimate the reduced elastic modulus, $E_{r,}$ and the hardness, H, of different phases. The three different phases of the NaOH activated system are clearly shown in Fig. 3. The same grid pattern was used for the NSH activated slag system, the only difference being the presence of two phases rather than three.

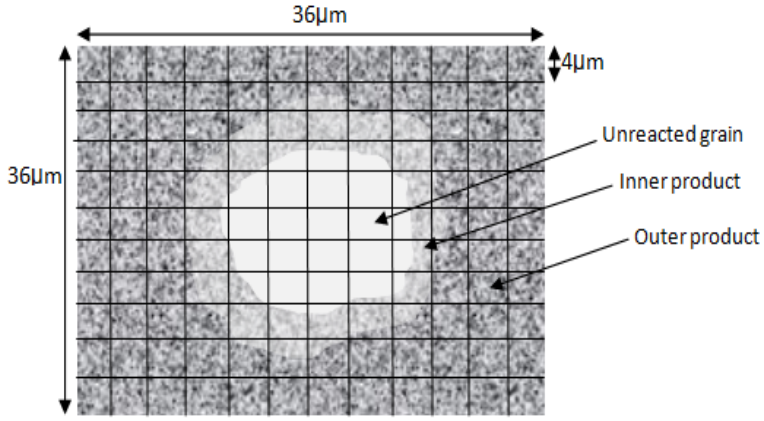

Fig. 3: Typical section of grid indent showing different phases of a hydrating system

The reduced modulus, hardness, and standard deviations are presented in Tables 1 and 2, respectively. Values from both the statistical nano-indentation and the manual indentation methods are shown. Both methods yielded very similar values with a few exceptions. In the manual method, the number of data points indented was fewer, but the location and the type of the phases indented were pre-defined. For example, a number of unreacted slag grains were selected based on the microstructure and the average E_r for the unreacted grain was calculated. The experiment was repeated by selecting either an outer product or an inner product to determine the E_r values. On the other hand, in the statistical analysis, once the grid pattern was selected, the automated indentation process indented 300 points in the microstructure, collecting the load-penetration curves. A histogram was then drawn using all of the 300 E_r values and hardnessa to designate the rage of E_r values and hardness for the unreacted slag grains, the inner product or the reaction ring and the outer products.

The result show that the E_r values of the outer product or the major binding gel was 25.02 ± 5.534 Gpa, 25.47± 5.818 Gpa and 28.64± 4.11 Gpa for 5 , 8 and 12 M sodium hydroxide activated slag, respectively. Only a slight increase in the E_r values were ocuured when the concentration of the NaOH solution increased. The E_r values of the outer product was 27.82 ± 10.737 and 30.27 ± 10. 067 Gpa for 1.5 and 2.5 SM NSH activated slag gel, respectively. There was a slight increase in the E_r values when the SM increased. A higher standard deviation in the E_r values of NSH activated gel was obtained.

Table 1: Average values of the different phases from the grid data points

Type	Phase	Er (GPa)	SD	#points	H (GPa)	SD	#points
5M	***Outer Product***	25.02	5.53	121	1.43	0.75	235
	Inner Product	41.42	3.56	65	6.15	0.88	26
	Unreacted grain	77.6	17.12	100	9.61	1.34	42
8M	***Outer Product***	25.47	5.82	160	1.24	0.51	251
	Inner Product	40.2	3.76	76	5.98	0.86	11
	Unreacted grain	70.14	15.43	36	10.18	0.97	38
12M	***Outer Product***	28.64	4.11	132	1.59	0.82	256
	Inner Product	41.55	3.78	100	6.16	0.94	27
	Unreacted grain	70.11	14.30	67	8.40	0.59	17
1.5MS	***Outer Product***	27.81	10.73	164	2.37	1.98	246
	Unreacted grain	85.14	23.61	74	13.21	2.99	46
2.5MS	***Outer Product***	30.27	10.06	155	2.64	1.76	246
	Unreacted grain	80.03	23.96	81	12.16	3.25	40

Table 1 shows that the E_r value was ~41GPa with a 3.5 SD for all concentrations of the NaOH activated slag and that the unreacted slag had an E_r value of approximately 70± 15 Mpa . The E_r values of the unreacted slag were higher, at about 80± 23.5, in the case of the sodium silicate activated slag.

The hardness value of the outer product varied from 1.2421± 0.0.512 to 1.59 ±0.0.8 for different concentrations of NaOH activator

Table 2: Average Er and H for manually indented points

Type	Phase	Er (GPa)	SD	H (GPa)	SD	# points
5M	*Outer Product*	28.8	6.25	1.26	0.52	12
	Inner Product	30.99	2.395	1.57	0.76	8
	Unreacted grain	52.42	11.19	3.92	1.6	7
8M	*Outer Product*	31.05	16.28	1.40	0.53	10
	Inner Product	36.11	7.64	1.70	0.96	8
	Unreacted grain	71.80	10.95	6.43	2.2	8
12M	*Outer Product*	33.304	5.07	1.45	0.48	12
	Inner Product	37.09	8.75	1.72	0.52	7
	Unreacted grain	69.4	7.42	5.89	1.7	7
1.5Ms	*Outer Product*	24.27	9.87	2.23	0.78	10
	Unreacted grain	61.84	7.64	6.34	1.52	11
2.5MS	*Outer product*	29.25	10.31	2.37	1.38	18
	Unreacted grain	72.44	12.017	7.12	1.95	16

CONCLUSION

The microstructure of a set of hardened 28 days ambient-cured alkali activated slag sytems was examined using an SEM to identify various phases present in each of them. The number of phases mainly depended on the activating alkali solution type and less on the concentration of the alkali. The microstructure features identified in sodium hydroxide activated systems were unreacted slag grains, a reaction ring around the slag grains (inner product), and a ground mass reaction gel that consisted of light and dark gray shades products (outer products). There were only two distinct phases present in NSH activated system; the unreacted slag grains and the new reaction product, ground mass gel (outer product). The E_r values obtained by the statistical automated nano-indentation and the manual methods showed clear differences between the unreacted slag, the inner product and the outer products in NaOH activated systems. Two clearly distinct E_r values were obtained in NSH activated slag.

ACKNOWLEDGMENT

The authors would like to acknowledge the finanacial support from the National Science Foundation through the CAREER grant award no.1055641

REFERENCES

Ben Haha, M., Le Saout, G. Winnefeld, F. and Lothenbach, B., 2012. Influence of slag chemistry on the hydration of alkali-activated blast-furnace slag — Part II: Effect of Al2O3. *Cem. Concr. Res.*, Volume 4, pp. 74-83.

Ben Haha, M., Le Saout, G. Winnefeld, F. and Lothenbach, B., 2011. Influence of activator type on hydration kinetics, hydrate assemblage and microstructural development of alkali activated blast-furnace slags.
Bernal, S. A., Gutierrez, R. M., Provis, J.L. and Rose, V., 2010. Effect of silicate modulus and metakaolin incorporation on the carbonation of alkali silicate-activated slags. *Cem. Concr. Res.*, Volume 40, pp. 898-907.
Davydov, D., Jirasek, M. and Kopecky, L., 2011. Critical aspects of nano-indentation technique in application to hardened cement paste. *Cem. Concr. Res.*, Volume 41, pp. 20-29
Diamond, S., 2006. The patch microstructure in concrete: The effect of superplasticizer. *Cem. Concr. Res.*, Volume 36, pp. 776-779
Fernandez-Jimenez, A., Palomo, J. G. and Puertas, F., 1999. Alkali-activated slag mortars Mechanical strength behavior. *Cem. Concr. Res.* , Volume 29, pp. 1313-1321.
Fernandez-Jimenez, A. P., 2005. Composition and microstructure of alkali activated fly ash binder: Effect of the activator. *Cem. Concr. Res.*, Volume 35, pp. 1984-1992
Lothenbach, B., Scrivener, K. and Hooton, R. D., 2011. Supplementary cementitious materials. *Cem. Concr. Res.*, Volume 41, pp. 217-229.
Miller, M., Bobko, C., Vandamme, M., and Ulm, F.J., 2008. Surface roughness criteria for cement paste nanoindentation. *Cem. Concr. Res*, Volume 38, pp. 467-476
Monteiro, P. J. M. and Mehta, P., 2006. *Concrete: Microstructure, properties and materials.* s.l.:McGraw-Hill.
Scrivener, K. L., Nonat, A., 2011. Hydration of cementitious materials, present and future. *Cem. Concr. Res.*, Volume 41, pp. 651-665
Shi, C. and Day, R. L., 1996. Some factors affecting early hydration of alkali-slag cements. *Cem. Concr. Res.*, Volume 26, pp. 439-441.
Wang, S.D, Pu, X., Scrivener, K. L. and Pratt, P. L., 1995. Alkali-activated slag cement and concrete: a review of properties and problems. *Adv. Cem. Res.* , Volume 7, pp. 93-102.